Exaiptasia diaphana from the Great Barrier Reef: a valuable resource for coral symbiosis research

Authors and Affiliations:

Dungan, Ashley M.[1]*§, Hartman, Leon[1,2§], Tortorelli, Giada[1], Belderok, Roy[1,3], Lamb, Annika M.[1,4], Pisan, Lynn[1,5], McFadden, Geoffrey I.[1], Blackall, Linda L.[1], van Oppen, Madeleine J. H.[1,4]

[1]School of Biosciences, University of Melbourne, Melbourne, VIC, Australia

[2] Swinburne University of Technology, Hawthorn, VIC, Australia

[3] Department of Freshwater and Marine Ecology, Institute for Biodiversity and Ecosystem Dynamics, University of Amsterdam, Amsterdam, The Netherlands

[4] Australian Institute of Marine Science, Townsville, QLD, Australia

[5] Kantonsschule Zug, Zug, Switzerland

[§]Equal first authors

*Correspondence:

Ashley M. Dungan

adungan31@gmail.com

Mobile: +61 403 442 289

ORCID: 0000-0003-0958-2177

Keywords: symbiosis, *Exaiptasia diaphana*, *Exaiptasia pallida*, model system, physiology, Symbiodiniaceae

Abstract

The sea anemone, *Exaiptasia diaphana*, commonly known as *Exaiptasia pallida* or *Aiptasia pallida*, has become increasingly popular as a model for cnidarian-microbiome symbiosis studies due to its relatively rapid growth, ability to reproduce sexually and asexually, and symbiosis with diverse prokaryotes and the same microalgal symbionts (family Symbiodiniaceae) as its coral relatives. Clonal *E. diaphana* strains from Hawaii, the Atlantic Ocean, and Red Sea are now established for use in research. Here, we introduce Great Barrier Reef (GBR)-sourced *E. diaphana* strains as additions to the model repertoire. Sequencing of the 18S rRNA gene confirmed the anemones to be *E. diaphana* while genome-wide single nucleotide polymorphism analysis revealed four distinct genotypes. Based on *Exaiptasia*-specific inter-simple sequence repeat (ISSR)-derived sequence characterized amplified region (SCAR) marker and gene loci data, these four *E. diaphana* genotypes are distributed across several divergent phylogenetic clades with no clear phylogeographical pattern. The GBR *E. diaphana* genotypes comprised three females and one male, which all host *Breviolum minutum* as their homologous Symbiodiniaceae endosymbiont. When acclimating to an increase in light levels from 12 to 28 µmol photons m^{-2} s^{-1}, the genotypes exhibited significant variation in maximum quantum yield of Symbiodiniaceae photosystem II and Symbiodiniaceae cell density. The comparatively high levels of physiological and genetic variability among GBR anemone genotypes makes these animals representative of global *E. diaphana* diversity and thus excellent model organisms. The addition of these GBR strains to the worldwide *E. diaphana* collection will contribute to cnidarian symbiosis research, particularly in relation to the climate resilience of coral reefs.

1 **Introduction**

1.1 Coral Reefs

The Great Barrier Reef (GBR) contains abundant and diverse biota, including more than 300 species of stony corals (Fabricius et al. 2005), making it one of the most unique and complex ecosystems in the world. In addition to its tremendous environmental importance, the GBR's social and economic value is estimated at $A56 billion, supporting 64,000 jobs and injecting $A6.4 billion into the Australian economy annually (O'Mahony et al. 2017).

Coral reef waters are typically oligotrophic, but stony corals thrive in this environment and secrete the calcium carbonate skeletons that create the physical structure of the reef. Corals achieve this through their symbiosis with single-celled algae of the family Symbiodiniaceae that reside within the animal cells and provide the host with most of its energy (Muscatine and Porter 1977). Additional support is provided by communities of prokaryotes, and possibly by other microbes such as viruses, fungi and endolithic algae living in close association with coral. This entity, comprising the host and its microbial partners, is termed the holobiont (Rohwer et al. 2002). During periods of extreme thermal stress, the coral-Symbiodiniaceae relationship breaks down. Stress-induced cellular damage creates a state of physiological dysfunction, which leads to separation of the partners and, potentially, death of the coral animal. This process, 'coral bleaching', is a substantial contributor to coral cover loss globally (Baird et al. 2009; De'ath et al. 2012; Eakin et al. 2016; Hughes et al. 2017; Hughes et al. 2018).

1.2 *Exaiptasia diaphana*

Model systems are widely used to explore research questions where experimentation on the system of interest has limited feasibility or ethical constraints. Established model systems, such as *Drosophila melanogaster* and *Caenorhabditis elegans*, have played crucial roles in the progress of understanding organismal function and evolution in the past 50 years (Davis 2004). The coral model *Exaiptasia diaphana* was formally proposed by Weis et al. (2008) as a useful system to study cnidarian endosymbiosis and has since achieved widespread and successful use.

E. diaphana is a small sea anemone (≤60 mm long) found globally within temperate and tropical marine shallow-water environments (Grajales and Rodriguez 2014). Originally positioned taxonomically within the genus *Aiptasia*, *E. diaphana* and twelve other *Aiptasia*

77 species were combined into a new genus, *Exaiptasia* (Grajales and Rodriguez 2014).
78 Although *Exaiptasia pallida* was proposed as the taxonomic name for the twelve
79 synonymized species, the International Commission on Zoological Nomenclature (ICZN)
80 ruled against this because the species epithet *diaphana* (Rapp 1829) predated *pallida* (Verrill
81 1864) and therefore had precedence according to the Principle of Priority (ICZN 2017).

82 *E. diaphana* was first used to study cellular regeneration (Blanquet and Lenhoff 1966), with
83 its systematic use in the study of cnidarian-algal symbioses dating back to 1976 when the
84 regulation of *in hospite* Symbiodiniaceae density was explored (Steele 1976). Since then,
85 studies using *E. diaphana* have focused on the onset, maintenance, and disruption of
86 symbiosis with Symbiodiniaceae (Belda-Baillie et al. 2002; Fransolet et al. 2014; Bucher et
87 al. 2016; Hillyer et al. 2017; Cziesielski et al. 2018). *E. diaphana* has also been used in
88 studies of toxicity (Duckworth et al. 2017; Howe et al. 2017), ocean acidification (Hoadley et
89 al. 2015), disease and probiotics (Alagely et al. 2011), and cnidarian development (Chen et
90 al. 2008; Grawunder et al. 2015; Carlisle et al. 2017). Key differences between corals and *E.*
91 *diaphana* are the absence of a calcium carbonate skeleton, the constant production of asexual
92 propagates, and the greater ability to survive bleaching events in the latter. These features
93 allow researchers to use *E. diaphana* to investigate cellular processes that would otherwise be
94 difficult with corals, such as those that require survival post-bleaching to track re-
95 establishment of eukaryotic and prokaryotic symbionts. Further, adult anemones can be fully
96 bleached without eliciting mortality, which is often difficult for corals, thus providing a
97 system for algal reinfection studies independent of sexual reproduction and aposymbiotic
98 larvae.

99 Three strains of *E. diaphana* currently dominate the research field as models for coral
100 research. H2 (female) was originally collected from Coconut Island, Hawaii, USA (Xiang et
101 al. 2013), CC7 (male) from the South Atlantic Ocean off North Carolina, USA (Sunagawa et
102 al. 2009) and RS (female, pers.comm., but see (Schlesinger et al. 2010)) collected from the
103 Red Sea at Al Lith, Saudia Arabia (Cziesielski et al. 2018). The majority of *E. diaphana*
104 resources have been developed from the clonal line, CC7, including reproductive studies
105 (Grawunder et al. 2015), transcriptomes (Sunagawa et al. 2009; Lehnert et al. 2012; Lehnert
106 et al. 2014) and an anemone genome sequence (Baumgarten et al. 2015). Prior work
107 evaluating multiple *E. diaphana* strains has shown variation in sexual reproduction
108 (Grawunder et al. 2015), Symbiodiniaceae specificity (Thornhill et al. 2013; Grawunder et al.

2015), and resistance to thermal stress (Bellis and Denver 2017; Cziesielski et al. 2018). However, Australian contributions to these efforts have been hampered as researchers have not had access to the established strains as import permits for alien species are difficult to secure.

The aim of the present work is to add GBR representatives to the existing suite of *E. diaphana* model strains. We describe the establishment and maintenance of four genotypes, including their provenance, taxonomy, maintenance, histology, physiology, and Symbiodiniaceae symbiont type. The results highlight characteristics that make GBR-sourced *E. diaphana* a valuable extension to this coral model, such as the physiological and genetic variability between genotypes, which is more representative of a global population. This foundation information will be useful to international researchers interested in using the GBR-sourced animals in their research and will give Australian researchers access to this valuable model.

2 **Methods**

2.1 Anemone acquisition and husbandry

Several pieces of coral rubble bearing anemones were obtained from holding tanks in the National Sea Simulator (SeaSim) at the Australian Institute of Marine Science and sent to Swinburne University of Technology, Melbourne (SUT) in late 2014. Additional anemones from the SeaSim were sent to the Marine Microbial Symbiont Facility (MMSF) at the University of Melbourne (UoM) in early 2016. Most material in the SeaSim tanks originates from the central GBR; therefore, this is the likely origin of the anemones. The SUT and UoM populations were consolidated at MMSF in early 2017 where they were segregated according to single polynucleotide polymorphism (SNP) analysis groupings (see below). Anemones were grown in 4 L polycarbonate tanks in reverse osmosis (RO) water reconstituted Red Sea Salt™ (RSS) at ~34 parts per thousand (ppt), and incubated without aeration or water flow at 26°C under lighting of 12-20 µmol photons m^{-2} s^{-1} (light emitting diode - LED white light array) on a 12h:12h light:dark cycle in a walk-in incubator. Anemones were fed *ad libitum* with freshly hatched *Artemia salina* (brine shrimp, Salt Creek, UT, USA) nauplii twice weekly. Tanks were cleaned each week after feeding by loosening algal debris with water pressure applied through disposable plastic pipettes, removing algal biomass, and complete water changes. When cleaning, ~25% of the anemones were cut into 2-6 fragments to promote population expansion through regeneration of the tissue fragments into whole anemones. Every third week, all anemones were transferred to clean tanks.

2.2 Anemone identity and genotyping

Anemone identity was determined by Sanger sequencing of the 18S rRNA gene. Genomic DNA (gDNA) was extracted from six whole anemones following the protocol described by Wilson et al. (2002), modified with a 15 min incubation in 180 µM lysozyme, and 30 s bead beating at 30 Hz (Qiagen Tissue-Lyser II) with 100 mg of sterile glass beads (Sigma G8772). The 18S rRNA genes were PCR amplified from all anemone samples using external Actiniaria-specific 18S rRNA gene primers 18S_NA, 5'-TAAGCACTTGTCTGTGAAACTGCGA-3' and 18S_NB, 5'-TAAGCACTTGTCTGTGAAACTGCGA-3' (Grajales and Rodriguez 2016) with 0.5 U 2x Mango Mix (Bioline), 2 µL of DNA template, 0.2 µM of each primer, and nuclease-free water up to 25 µL. PCR conditions consisted of initial denaturation at 94°C for 5 min, 35 cycles of 94°C for 45 s, 55°C for 45 s, and 72°C for 45 s followed by a final extension at 72°C for 5 min. PCR

products were purified with an ISOLATE II PCR and Gel Kit (Bioline, BIO-52059) according to the manufacturers guidelines, and supplied to the Australian Genome Research Facility (AGRF) for Sanger sequencing with the external primers and four internal primers: 18S_NL, 5'-AACAGCCCGGTCAGTAACACG-3', 18S_NC 5'-AATAACAATACAGGGCTTTTCTAAGTC-3', 18S_NY 5'-GCCTTCCTGACTTTGGTTGAA-3', and 18S_NO 5'-AGTGTTATTGGATGACCTCTTTGGC-3'. The raw 18S reads were aligned in Geneious (v 10.0.4) (Kearse et al. 2012) to produce the near-complete 18S rRNA gene sequence, which was evaluated by BLASTn (Altschul et al. 1990) to identify the anemones.

For genotyping, DNA was extracted as described above from 23 whole anemones or their tentacles and sent to Diversity Arrays Technology Pty Ltd (Canberra, Australia) for DArT next-generation sequencing (DArTseq). DArTseq combines complexity reduction and next generation sequencing to generate genomic data with a balance of genome-wide representation and coverage (Cruz et al. 2013). Complexity reduction was achieved by using restriction endonucleases to target low-copy DNA regions. These regions were then sequenced using Illumina HiSeq2500 (Illumina, USA) with an average read depth exceeding 20x. The data were processed by DArT Pty Ltd to remove poor quality sequences and to ensure reliable assignment of sequences to samples. DArTsoft14 was then used to identify SNPs at each locus as homozygous reference, homozygous alternate or heterozygous for each individual (Melville et al. 2017). Monomorphic loci, loci with <100% reproducibility or missing values were removed in the R package, dartR, to improve the quality of and reduce linkage within the dataset; this reduced the dataset from 8288 loci to 1743 loci (R Core Team 2013; Gruber et al. 2017).

Euclidean distances between individual anemones, based on differences in the allele frequencies at each of the SNP loci, were calculated from the reduced SNP dataset in dartR, then viewed as a histogram and printed into a matrix in RStudio. Although the genetic distance between individuals of the same genotype should be zero, small differences may occur due to sequencing errors and somatic mutations. The genetic distance between individuals of different genotypes will be larger than that within individuals. Therefore, the genetic distances among individuals from several genotypes should form a bi- or multi-modal distribution; one peak with a relatively small mean represents genetic distances between pairs of individuals of the same genotype, another represents inter-genotypic distances with a larger mean. The inter-

genotypic distribution can be multi-modal because different pairs of genotypes can differ by different amounts. Note that two samples from the same individual were genotyped to determine methodological error rates and verify the baseline for clonality. A principal coordinates analysis was performed and plotted in dartR to visualize the genotype assignments.

To compare the phylogenetic relationship of the GBR-sourced anemones with the previously described clonal lines, we used a set of four *Exaiptasia*-specific inter-simple sequence repeat (ISSR)-derived sequence characterized amplified region (SCAR) markers developed by Thornhill et al. (2013) and an additional six *Exaiptasia*-specific gene loci (Bellis and Denver 2017). gDNA was extracted from five animals of each genotype, as described above, and amplified with each of the four SCAR marker (3, 4, 5, and 7) and gene primer pairs (Thornhill et al. 2013; Bellis and Denver 2017). PCR solutions for each marker contained 0.5U MyTaq HS Mix polymerase (Bioline), 1 µL of DNA template, 0.4 µM of each primer, and nuclease-free water up to 25 µL. Thermocycling consisted of an initial denaturation at 94°C for 1.5 min, 35 cycles of 94°C for 1 min, 56°C for 1 min, and 72 °C for 1.5 min followed by a final extension at 72°C for 5 min. Amplified products were purified and sequenced in forward and reverse directions at AGRF. Sequences were aligned and edited in Geneious version 2019.2. Substantial non-specific binding of the SCAR marker 7 primers generated unusable sequence data. Further, the forward and reverse sequences from two anemone genotypes that were heterozygous for two or more indels at different points in the sequences of SCAR markers 3 (anemone AIMS1) and 4 (anemones AIMS2-4) could not be aligned and this prohibited the inclusion of those loci from analyses. Therefore, only sequence data from SCAR marker 5 was used for phylogenetic analyses. For the six *Exaiptasia*-specific gene loci, only AIPGENE19577, Atrophin-1-interacting protein 1 (AIP1) contained heterozygous indels or non-specific binding of the forward primer.

For each genotype, the SCAR marker 5 sequences and each of the six *Exaiptasia*-specific gene loci of the clonal replicates were aligned and a consensus sequence was generated. For the SCAR marker, the consensus sequences were aligned with twelve reference sequences from Thornhill et al. (2013) and three experimental anemone sequences (Grawunder et al. 2015), while the *Exaiptasia*-specific gene sequences were aligned with five reference sequences from Bellis and Denver (2017). Each alignment was used to create a phylogenetic tree using the Maximum Likelihood method and General Time Reversible model (Nei and Kumar 2000) in MEGA X (Kumar et al. 2018). Topology, branch length, and substitution

rate were optimized, and branch support was estimated by bootstrap analysis of 1000 iterations.

2.3 GBR anemone gender determination

Over a period of two months, several anemone individuals from each genotype were reared to a pedal disk diameter of ~7 mm. One animal per genotype was anesthetized in a 1:1 solution of 0.37 M magnesium chloride and filter-sterilized RSS (fRSS) for 30 min, dissected and viewed under a stereo microscope (Leica MZ8) to confirm the presence of gonads. When gonads were observed, one animal per genotype was anesthetized as described above, fixed in 4% paraformaldehyde in 1x PBS (pH 7.4) overnight, washed three times in 1x PBS and processed by the Biomedical Histology Facility of The University of Melbourne. Samples were embedded in paraffin and 7 µm transverse sections were cut (see supplemental information Online Resource 1 for histological processing). Slides were stained with hematoxylin and eosin (H&E) and viewed under a compound microscope (Leica DM6000B).

2.4 Symbiodiniaceae

The ITS2 region of Symbiodiniaceae gDNA was analyzed by metabarcoding to determine the Symbiodiniaceae species associated with the GBR-sourced anemones. gDNA extracted from three animals of each genotype, as described above, was amplified in triplicate with the ITS-Dino (forward; 5'-TCGTCGGCAGCGTCAGATGTGTATAAGAGACAGGTGAATTGCAGAACTCCGTG-3') (Pochon et al. 2001) and its2rev2 (reverse; 5'-GTCTCGTGGGCTCGGAGATGTGTATAAGAGACAGCCTCCGCTTACTTATATGCTT-3') (Stat et al. 2009) primers modified with Illumina adapters. PCRs included 0.5 U MyTaq HS Mix polymerase (Bioline), 1 µL of DNA template, 0.25 µM of each primer, and nuclease-free water up to 20 µL. Thermocycling consisted of an initial denaturation at 95.0 °C for 3 min, 35 cycles at 95.0 °C, 55.0 °C and 72.0 °C for 15 sec each, and 1 cycle at 72 °C for 3 min. Library preparation on pooled triplicates and Illumina MiSeq sequencing (2x250 bp) was performed by the Ramaciotti Centre for Genomics at the University of New South Wales, Sydney. Raw, demultiplexed MiSeq read-pairs were joined in QIIME2 v2018.4.0 (Bolyen et al. 2018). Denoising, chimera checking, and trimming was performed in DADA2 (Callahan et al. 2016). The remaining sequences were clustered into operational taxonomic units (OTUs) at 99% sequence similarity using closed-reference OTU picking in vsearch

(Rognes et al. 2016). A taxonomic database adapted from Arif et al. (2014) was used to seed the OTU clusters and for taxonomic classification.

2.5 Anemone and Symbiodiniaceae physiological properties

Physiological assessments were performed on anemones maintained in a healthy, unbleached state for over two years. Three of the four anemone genotypes named AIMS2, AIMS3, and AIMS4, with oral disk diameters of 3-4 mm were transferred from the original holding tanks in the walk-in incubator and randomly distributed between three replicate (by genotype) 250 mL glass culture containers containing RSS. Anemones of this size were chosen as they were considered sexually immature (Muller-Parker et al. 1990; Grawunder et al. 2015) and therefore variability in sexual development or gonadal reserves were unlikely to influence the results. AIMS1 was excluded from long-term assessment as it had poor survival at densities required for the analyses.

Glass culture containers were transferred from the walk-in incubator to experimental growth chambers (Taiwan HiPoint Corporation model 740FHC) fitted with red, white, and infrared LED lights. Initial light levels were set at 12 µmol photons m^{-2} s^{-1} (HiPoint HR-350 LED meter) to correspond with the walk-in incubator conditions and ramped up to 28 µmol photons m^{-2} s^{-1} over a period of 72 h on a 12 h:12 h light:dark cycle to approximate experimental conditions reported in *E. diaphana* literature (Online Resource 2; Fransolet et al. 2014; Hoadley and Warner 2017). While the commonly used *E. diaphana* strains (CC7, H2, RS) are often maintained at >50 µmol photons m^{-2} s^{-1} (pers. comm.), the GBR strains appeared healthier, with extended bodies and open tentacles, at lower light intensities. The anemones were maintained in RSS, fed *A. salina* nauplii and cleaned as described above. The pH, salinity and temperature of the water and applied light levels were monitored thrice weekly and were stable over time: 8.14±0.02, 35.0±0.04 ppt, 25.77±0.07°C and 28.08±0.12 µmol photons m^{-2} s^{-1}, respectively. Culture containers were placed on a single incubator shelf and randomly rearranged after each clean to minimize confounding by position.

The maximum dark adapted quantum yield (Fv/Fm) of photosystem II (PSII) of *in hospite* Symbiodiniaceae provides an indication of photosynthetic performance and is useful as a bio-monitoring tool (Howe et al. 2017). Fv/Fm is measured as the difference in fluorescence produced by PSII reaction centers when either saturated by intense light (Fm) or in the absence of light (Fo), versus Fm (i.e. (Fm–Fo)/Fm, or Fv/Fm). Symbiodiniaceae Fv/Fm was

280 measured weekly over nine weeks for each culture container after 4 hr into the incubator light
281 cycle and 30 mins dark adaption using imaging pulse amplitude modulated (iPAM)
282 fluorometry (IMAG-MAX/L, Waltz, Germany). Settings for all measurements were:
283 saturating pulse intensity 8, measuring light intensity 2 with frequency 1, actinic light
284 intensity 3, damping 2, gain 2. Average Fv/Fm values for each dish were calculated from
285 readings taken on three to five anemones (Online Resource 3).

286 Anemones from each culture container were individually homogenized in a sterile glass
287 homogenizer in 1 mL fRSS, and 100 µL of homogenate was collected and stored at -20 °C
288 for total protein measurement. The remaining 900 µL of homogenate was centrifuged at 5000
289 *g* for 5 min at 4°C to pellet the Symbiodiniaceae while leaving the anemone cells in
290 suspension. A volume of 100 µL of supernatant was collected and stored at –20 °C for host
291 protein measurement. The pelleted Symbiodiniaceae were twice washed with 500 µL fRSS
292 and centrifuged at 5000 *g* for 5 min at 4 °C, and the final pellet resuspended in 500 µL fRSS
293 and stored at –20 °C for Symbiodiniaceae counts. Triplicate cell counts (cells mL^{-1}) were
294 completed within 48 hrs of sample collection on a Countess II FL automated cell counter
295 (Life Technologies) and normalized to host protein (mg mL^{-1}). This process was repeated 15
296 times over the course of nine weeks for a total of 45 replicates per genotype.

297 Samples for protein analysis stored at –20 °C (see above) were used within one month of
298 collection to determine total and host protein (mg mL^{-1}) by the Bradford assay (Bradford
299 1976) against bovine serum albumin standards (Bio-Rad 500-0207). Readings were taken at
300 595 nm (EnSpire microplate reader MLD2300).

301 Fv/Fm values and Symbiodiniaceae cell densities were assessed for genotype-specific
302 responses. All variables were tested for normality and homoscedasticity prior to parametric
303 analyses, which were completed in R (v 3.6.0). Genotypic responses of Fv/Fm were
304 compared using a linear model in the R package nlme (Pinheiro et al. 2017) to evaluate
305 independent and interaction relationships between the factors of genotype and time. F-
306 statistics were obtained using the analysis of variance (ANOVA) function, nlme, and
307 pairwise *post hoc* analyses were performed using the glht function in the R package
308 multcomp (Hothorn et al. 2016) with Tukey's correction for multiple comparisons.
309 Symbiodiniaceae cell densities were pooled across time by genotype and analyzed with a
310 one-way ANOVA with a *post hoc* Tukey test to determine pairwise significance.

Results and Discussion

3.1 Anemones

The assembled 18S rRNA gene sequences of two genotypes (AIMS2 and AIMS4) covered 1591 and 1594 bp, respectively, with two mismatches between the sequences. BLASTn against the NCBI database identified the samples as either *Aiptasia pulchella* or *Exaiptasia pallida*. *A. pulchella* has been synonymised with *E. pallida* (Grajales and Rodríguez, 2014). However, since *E. diaphana* has precedence (ICZN 2017), all samples were designated *E. diaphana*.

Four SNP genotypes of *E. diaphana*, which were of GBR-origin but AIMS-sourced, were identified and designated AIMS1, AIMS2, AIMS3 and AIMS4 (Fig. 1). The clonal distribution of Euclidean distances was identified (range of 0-9.61) and pairs of individuals with Euclidean distances within this distribution were inferred to have the same genotype (Online Resource 3-4). The Euclidean distance between the originally named Ed.11a and Ed.11b (replicates from the same individual; assigned AIMS3) is in the upper percentiles of the defined clonal distribution, confirming this cut-off is valid.

Using phylogenetic analysis with our data, previously described SCAR marker 5, and the *Exaiptasia*-specific gene sequence data (Thornhill et al. 2013; Grawunder et al. 2015; Bellis and Denver 2017), we placed the GBR anemones into a phylogeographical context. The alignment of SCAR5 sequences was 706 bp long and contained 19 variable nucleotide positions (Fig. 2), while the concatenated *Exaiptasia*-specific gene sequences were 3276 bp long with 92 variable nucleotide positions (Fig. 3).

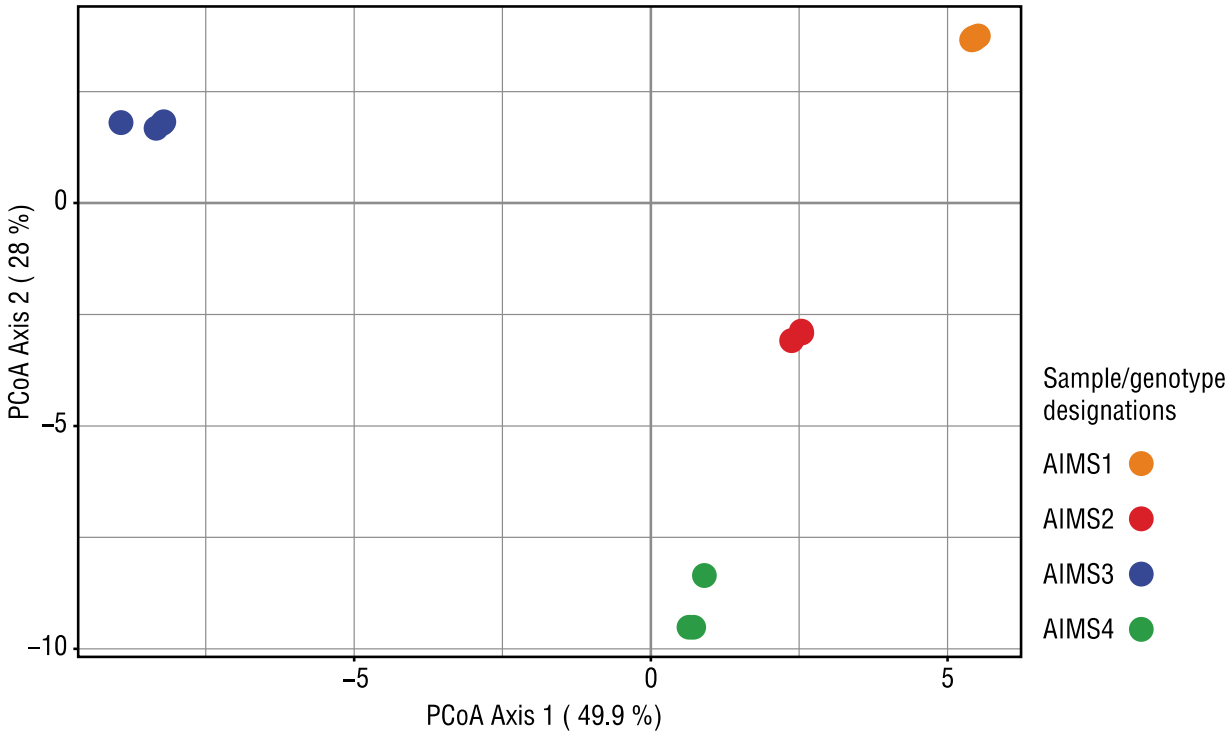

Figure 1: PCoA ordination of *Exaiptasia diaphana* genotypes based on Euclidean genetic distance measurements of SNP data using allele frequencies within individuals to calculate genetic distance between them (AIMS1, n=8; AIMS2, n=5, AIMS3, n=7; AIMS4, n=3). Individuals of the same genotype may overlap in the plot due to their high similarity.

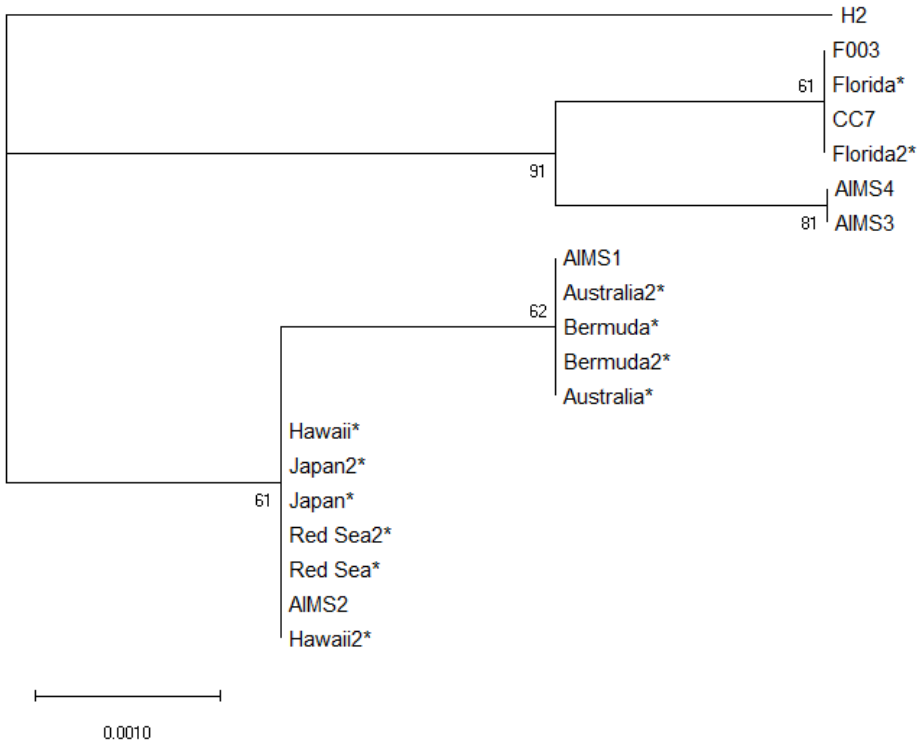

337

338 **Figure 2:** The phylogenetic relationships of the four GBR *E. diaphana* compared to other conspecific anemones
339 sampled across the globe inferred from SCAR marker 5 using the Maximum Likelihood method and General
340 Time Reversible model (Nei and Kumar 2000). The tree with the highest log likelihood is shown with bootstrap
341 values next to the nodes. Initial trees for the heuristic search were obtained automatically by applying the
342 Maximum Parsimony method. The tree is drawn to scale, with branch lengths measured in the number of
343 substitutions per site. This analysis involved 19 *E. diaphana* sequences and 706 nucleotide positions were
344 included. Sequences were from our *E. diaphana* genotypes (AIMS1-4), globally distributed *E. diaphana* from

Thornhill et al. (2013), indicated with an asterisk, and from experimental genotypes CC7, H2, and F003 (Grawunder et al. 2015).

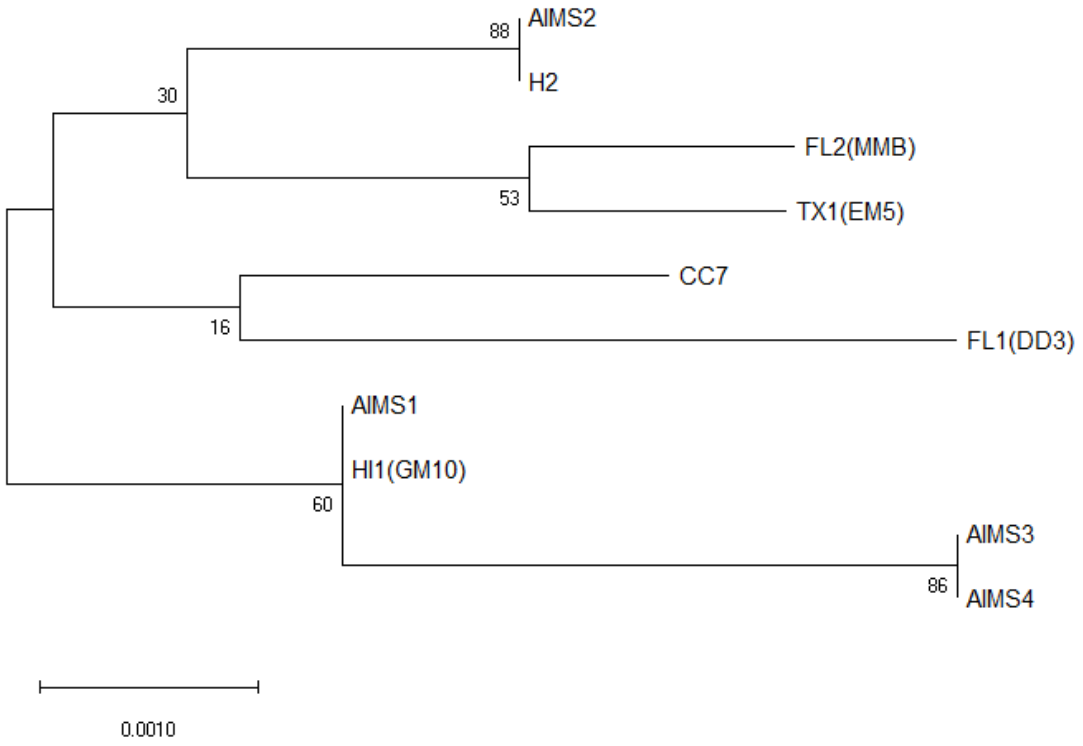

Figure 3: The phylogenetic relationships of the four GBR *E. diaphana* (AIMS1-4) compared to other experimental anemones using the Maximum Likelihood method and General Time Reversible model (Nei and Kumar 2000) on six concatenated *Exaiptasia*-specific gene sequences (Bellis and Denver 2017). Data from Bellis and Denver (2017) was downloaded from GenBank (accession numbers KU847812-KU847847); tree branches are named as strain name followed by the alternative strain name in parentheses. Bootstrap values are shown next to the nodes. Initial trees for the heuristic search were obtained automatically by applying the Maximum Parsimony method. The tree is drawn to scale, with branch lengths measured in the number of substitutions per site. This analysis involved 10 *E. diaphana* sequences and 3267 nucleotide positions were included.

Based on SCAR marker data, *E. diaphana* is regarded as a single pan-global species with two distinct genetic lineages: one from the USA Atlantic coast, and a second consisting of all other *E. diaphana* worldwide (Thornhill et al. 2013). The SCAR5 allele sequenced for genotype AIMS1 is identical with that from anemones originally collected off Heron Island, Australia and Bermuda, while that of AIMS2 is nearly identical to (two base pair differences, both with an ambiguous base) samples from Hawaii, Japan and the Red Sea. AIMS3 and AIMS4 are most closely related to anemones from Florida and North Carolina, USA and are identical to one another in this region.

Similar to Bellis and Denver (2017), our data from the *Exaiptasia*-specific gene sequences (Fig. 3) show that, while anemone strains are genetically distinct, there is not a strong

366 phylogenetic separation between individuals collected from distant geographic locations.
367 Again, AIMS1-4 show genetic variation, with AIMS1 and AIMS2 clustering with anemone
368 strains originating from Coconut Island, Hawaii, USA which were collected independently in
369 1979 and early 2000's, respectively. Corresponding with the SCAR5 loci data, AIMS3-4 have
370 near identical sequences in the sequenced regions (differences at two heterozygous sites).
371 Because the available data for SCAR5 and the *Exaiptasia*-specific gene targets are not from all
372 the same individuals, with the exception of CC7 and H2, comparing between the two is not
373 feasible. However, given the larger number of alignment positions and variable sites in the
374 gene regions with better PCR results, we suggest that researchers use the primers presented in
375 Bellis and Denver (2017) for future comparisons between *E. diaphana* used in experiments.
376 The diversity that is revealed by whole genome SNP analysis (Fig. 1) is hidden with these six
377 *Exaiptasia*-specific gene sequences, suggesting that there are more informative loci not yet
378 published for *E. diaphana* genotyping.

379 There are several possible explanations for the AIMS1-4 anemones to be spread throughout
380 the phylogenetic trees. First, due to small sample sizes at all sampling locations, only a subset
381 of the alleles have been sampled and location-specific alleles may have been missed. Second,
382 it is conceivable that the GBR is the source of all other *E. diaphana* populations and founder
383 effects mean that other geographic locations have *E. diaphana* that represent only some of the
384 diversity. Third, it is possible that the GBR *E. diaphana* was a distinct lineage and the GBR
385 has since been invaded by *E. diaphana* from other lineages, or the GBR lineage has been
386 introduced elsewhere. Introductions over such vast spatial scales may have occurred via ship
387 ballast water or attached to ships hulls in fouling biomass, which is notorious for transporting
388 marine life and introducing invasive animals and plants, or via the aquarium trade or marine
389 farms. Irrespective of the cause, the genetic variation across the four GBR genotypes is more
390 representative of global diversity than a single localized population. Because strain-specific
391 responses to environmental variables have been observed among *E. diaphana* strains (Bellis
392 and Denver 2017; Cziesielski et al. 2018) it is critical to conduct experiments, such as those
393 regarding climate change and symbiosis, with a diverse set of individuals, much like the
394 diversity presented by the GBR-sourced *E. diaphana*.

395 3.2 Symbiosis with Symbiodiniaceae

396 According to a global survey by Thornhill et al. (2013), Pacific Ocean *E. diaphana* (e.g., H2)
397 associate exclusively with the Symbiodiniaceae species *Breviolum minutum* (formerly ITS2

type *Symbiodinium* Clade B, sub-clade B1 (LaJeunesse et al. 2018)). Symbiodiniaceae sequences from the four GBR *E. diaphana* genotypes were almost exclusively *Breviolum minutum* (>99.6%), thus concurring with Thornhill et al. (2013). Two as-yet unnamed species of *Breviolum* (previously known as *Symbiodinium* sub-clades B1i and B1L (LaJeunesse et al. 2018)) were also identified in *E. diaphana*. Their very low relative abundance suggests they are either intragenomic variants or rare strains.

Stable endosymbiotic relationships between corals and Symbiodiniaceae are vital for sustaining coral reef ecosystems; this symbiotic relationship is the focus of much coral reef research. Interestingly, while the GBR anemones are genetically diverse, all host *B. minutum* as their sole Symbiodiniaceae. Given this, we may be able to investigate the symbiotic mechanisms of the host-algal relationship and answer questions about this symbiosis that are not restricted by anemone strain.

3.3 Sex of *E. diaphana*

E. diaphana lacks obvious gender defining morphological features, but gonad development is related to size (Chen et al. 2008). Partially developed oocytes with germinal vesicles (*i.e.*, the nucleus of an oocyte arrested in prophase of meiosis I) were observed in histological slides in animals of AIMS1, AIMS3 and AIMS4 and Stage V spermaries were observed in AIMS2 (Fig. 4). In Stage V, the spermary is made up of a mass of spermatozoa with their tails facing in the same direction. In this advanced stage the spermatozoa are capable of fertilization (Fadlallah and Pearse 1982; Goffredo et al. 2012). While most AIMS1 anemones grew to only 5 mm in pedal disk diameter, gonad development was still observed. Differences between male and female gonads were present but were macroscopically cryptic. Male gonads have been observed to be smaller and lighter colored than female gonads in *E. diaphana* (Grawunder et al. 2015), and this was also the case in the GBR-sourced females (AIMS1, AIMS3 and AIMS4) and male (AIMS2) *E. diaphana*.

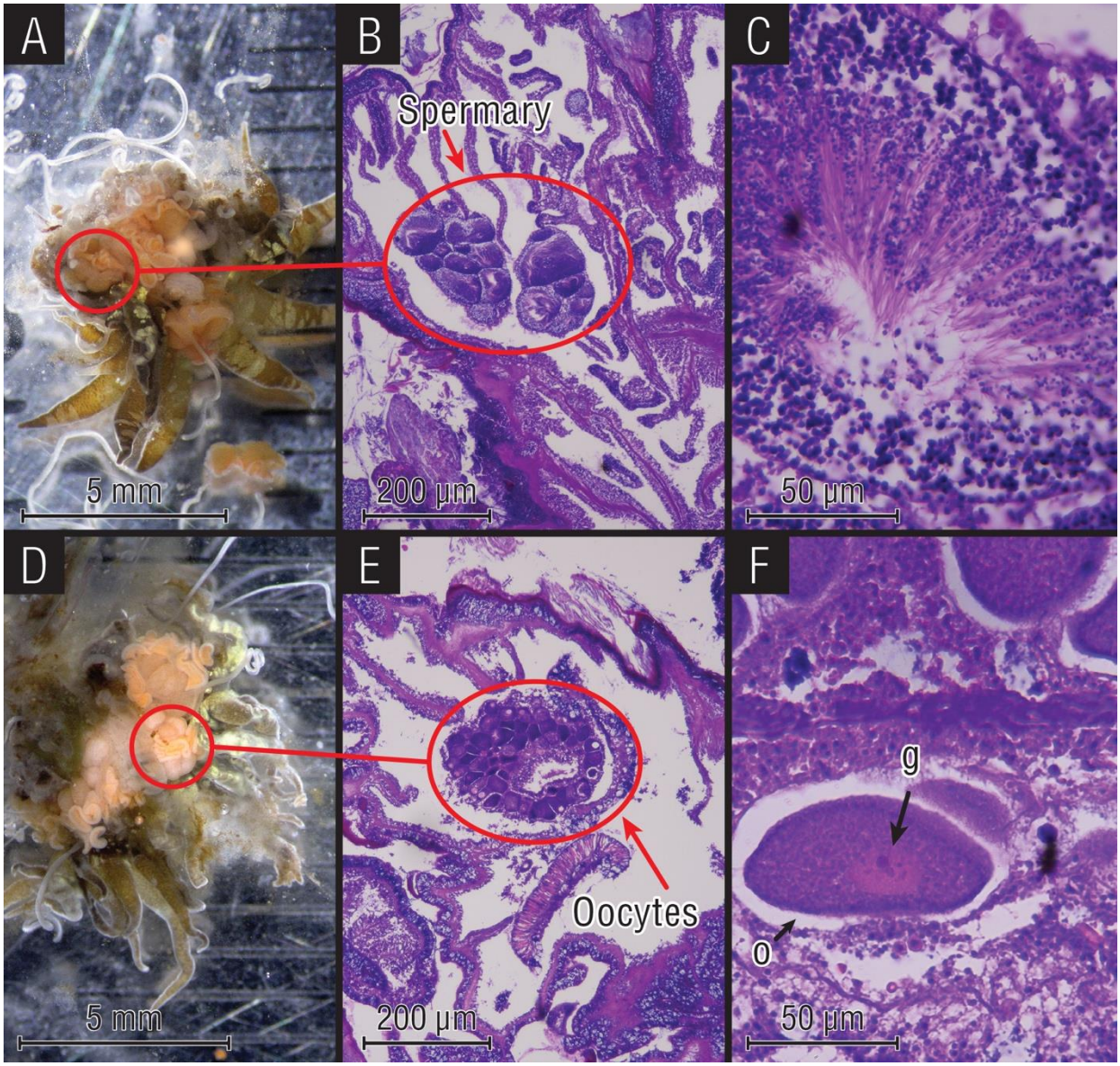

Figure 4: (A) Dissected male anemone with developing gonads (AIMS2, ~1 cm pedal disk diameter); (B) H&E stained tissue section, with stage 5 spermary; (C) Increased magnification of stage 5 spermary; (D) dissected female anemone with developed gonads (AIMS4, ~1 cm pedal disk diameter); (E) H&E stained tissue section with oocytes; (F) increased magnification of female gonad with developing oocyte (o) and germinal vesicle (g).

3.4 *E. diaphana* and Symbiodiniacease Physiology

Throughout the nine-week evaluation period all *E. diaphana* maintained a healthy appearance, including *in hospite* Symbiodiniaceae, tentacle extension, active feeding of *A. salina* nauplii and asexual propagation. Average Symbiodiniaceae cell densities (normalized to host protein) were significantly different between genotypes (one-way ANOVA ($F_{(3,200)}$=3.985, p=0.00872; Fig. 5; Online Resource 6). All anemones hosted ~10^6 Symbiodiniaceae cells mg^{-1} host protein, which is comparable to densities reported for other lab cultured model *E. diaphana* systems (Hoadley et al. 2015; Hawkins et al. 2016b; Rädecker et al. 2018) and is similar to Symbiodiniaceae cell densities found in scleractinian corals (Cunning and Baker 2014; Ziegler et al. 2015; Kenkel and Bay 2018). The only statistically significant difference observed was the lower Symbiodiniaceae cell density of AIMS2 (mean ± SE; 7.17 x 10^6 ± 2.73 x 10^5 per mg host protein, n=66) compared to AIMS3 (mean ± SE; 8.46 x 10^6 ± 2.96 x 10^5 per mg host protein, n=66) (Fig. 5).

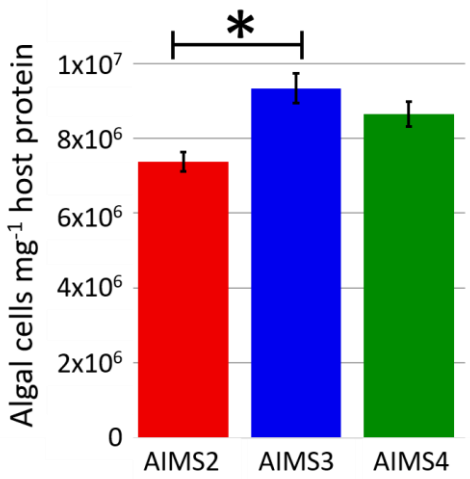

Figure 5: Mean ± 1SEM Symbiodiniaceae cells mg^{-1} host protein for GBR *E. diaphana* genotypes AIMS2-4. Seventy-five AIMS2-4 anemones were collected over a period of nine weeks. Asterisk indicates significant difference, $p<0.05$.

All genotypes experienced a nearly identical drop in Fv/Fm after the light intensity was increased from 12 to 28 µmol photons m^{-2} s^{-1}, from an average of 0.53 on day 0, to an average of 0.40 by day 21 (Online Resource 7; Fig. 6). However, by day 36 the Fv/Fm values had returned to initial levels.

Changes in environmental variables, such as light intensity, are known to influence photobiological behavior of Symbiodiniaceae (Wangpraseurt et al. 2014; Hoadley and

Warner 2017). A change in light intensitycan alter photosynthetic efficiency as measured by Fv/Fm (Hoadley and Warner 2017). GBR anemone genotypes AIMS2, AIMS3 and AIMS4 took 36 d to recover from this environmental change and return to photosynthetic efficiencies recorded at 12 µmol photons m^{-2} s^{-1}. Such information is critical for planning and conducting symbiosis studies. Most of the statistical differences between the genotypes occurred between days 19-28 (Online Resource 8) when Fv/Fm was lowest. Once acclimated at day 36, average Fv/Fm values for all genotypes were not significantly different (mean ± SE; 0.479 ± 0.003, n=80), except for day 40 where the Fv/Fm of AIMS2 was significantly higher than AIMS3 (p=0.0068).

As all the GBR-sourced anemones harbour *Breviolum minutum* as their homologous symbiont type, it is not unexpected that the different genotypes would have similar maximum Fv/Fm values. Furthermore, similar Fv/Fm values have been reported for other anemones hosting homologous *B. minutum* (Hawkins et al. 2016b; Hillyer et al. 2017). However, it is noteworthy that AIMS2 is not only able to recover its photosynthetic efficiency quicker from changing light levels with a milder dip in Fv/Fm values (Fig. 6), but also hosts significantly fewer Symbiodiniaceae cells mg^{-1} host protein compared to AIMS3 (Fig. 5). Reductions in the maximum quantum yield of photosystem II (PSII) (Fv/Fm) is observed in the early phases of natural bleaching events (Gates et al. 1992; Franklin et al. 2004) and the ability of AIMS2 to maintain a higher efficiency of PSII photochemistry during changing environmental conditions could translate into higher thermal tolerance (Suggett et al. 2008; Ragni et al. 2010; Goyen et al. 2017).

These individuals are genetically diverse based on SNP genotyping (Fig. 1) and phylogenetic analysis (Fig. 2-3); the phenotypic feature of AIMS2 being more robust to increasing light levels compared to AIMS3 and AIMS4 could be a host genotypic effect. There is evidence that genetic variation of *E. diaphana* may influence holobiont response to heat stress, though this hypothesis has only been tested on anemone strains hosting different Symbiodiniaceae species (Bellis and Denver 2017; Cziesielski et al. 2018) or after experimentally bleaching anemones and inoculating with new heterologous algal cells (Perez et al. 2001). As we have four GBR-sourced *E. diaphana* genotypes with inherent genetic variability and all contain *B. minutum* as their homologous symbiont, we will be able to explore the roles of host and symbiont in the bleaching response.

An alternative possibility is that the GBR anemones' Symbiodiniaceae communities comprise diversity that may be hidden under the resolution of the ITS2 sequences we used in this experiment, which are driving the differences in photosynthetic efficiency. Distinct strains of a given Symbiodiniaceae species can have different susceptibilities to thermal stress (Ragni et al. 2010; Howells et al. 2012; Hawkins et al. 2016a), with evidence that these variations in thermal optima can drive host-Symbiodiniaceae interactions (Hawkins et al. 2016a). Thus, varying rates of recovery of Fv/Fm among Symbiodiniaceae strains (Fig. 6) could provide a mechanism for the emergence of novel and potentially resilient cnidarian-Symbiodiniaceae associations in a rapidly warming environment.

Another explanation for the physiological differences between AIMS2 and AIMS3 (Fig. 5) is through algal cell density moderation by the host. It is thought that the coral host controls Symbiodiniaceae densities through nitrogen limitation (Falkowski et al. 1993), although the mechanisms are not well understood (Davy et al. 2012). During temperature stress, higher densities of Symbiodiniaceae have been implicated in increasing the susceptibility of corals to bleaching, potentially as a result of the higher reactive oxygen species production relative to corals' antioxidant capacity (Cunning and Baker 2012). Altogether, our data suggest that AIMS2, which hosted fewer algal symbionts and recovered from increased light conditions faster than AIMS3, may be more resilient to thermal stress, while AIMS3 could be more susceptible to bleaching with AIMS4 as an intermediate.

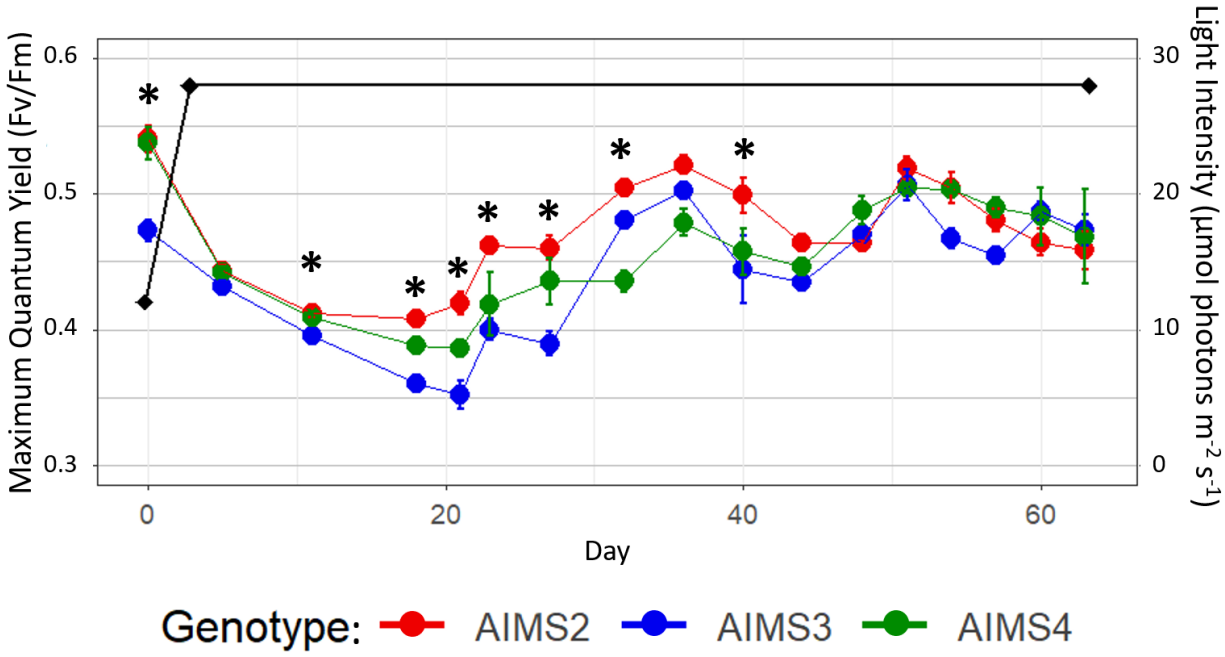

Figure 6: Fv/Fm measurements for anemones AIMS2, AIMS3 and AIMS4 over a 63-day period. Anemones were initially exposed to light levels (black line) of 12 µmol photons m^{-2} s^{-1} (12:12 light:dark cycle), which were then increased to 28 µmol photons m^{-2} s^{-1} over a 72 h period. Day 0 marks the start of light ramping. The anemones took ~35 d to recover their maximum quantum yield due to the increase in light exposure although Symbiodiniaceae densities remained largely constant. Asterisks indicate significant differences in pairwise comparisons between genotypes at given time points (Online Resource 8)

4 Conclusions and Future Directions

The study of *E. diaphana* anemones of GBR origin described here provide further information on phenotypic and genetic variation within this species and complements data on the more widely used *E. diaphana* strains CC7 and H2. The four genotypes in our collections capture a level of genetic diversity previously observed in animals from different oceans and are therefore a hugely valuable addition to the model collections. Knowledge of their characteristics enhances and broadens the potential of this model system for climate change research in corals, particularly, but not exclusively, for Australian researchers. We propose future research on this collection should focus on characterization of associated prokaryotes to explore the value of these animals as models for coral-prokaryote symbiotic interactions. Future research in cnidarian-prokaryotic interactions would be enhanced by the development of axenic (germ-free) or gnotobiotic (with a known microbial community) *E. diaphana* cultures. They could be used to test the influence of native and non-native microbiota on holobiont performance, and the ability of probiotic inocula to support animal health during stress (Alagely et al. 2011; Damjanovic et al. 2017; Rosado et al. 2018).

5 Acknowledgments

This research was funded by Australian Research Council Discovery Project grants DP160101468 (to MJHvO and LLB) and DP160101539 (to GIM and MJHvO). We thank Lesa Peplow for facilitating transport of the initial anemone cultures from AIMS to SUT and UoM and Rebecca Alfred from SUT for initial anemone culture maintenance. We acknowledge Anton Cozijnsen, Keren Maor-Landaw, Samantha Girvan, Ruby Vanstone and Gabriela Rodriguez from University of Melbourne for assisting with anemone husbandry and Laura Leone, Lisa Foster, and Lona Dinha from the Melbourne Histology Platform for histological sample preparation and sectioning. SCAR marker reference sequences were provided by Dan Thornhill and Liz Hambleton (AG Guse Lab, Centre for Organismal Studies (COS), Universität Heidelberg). MJHvO acknowledges Australian Research Council Laureate Fellowship FL180100036.

535 Alagely A, Krediet CJ, Ritchie KB, Teplitski M (2011) Signaling-mediated cross-talk
536 modulates swarming and biofilm formation in a coral pathogen Serratia marcescens
537 ISME J 5:1609-1620 doi:10.1038/ismej.2011.45
538 Altschul SF, Gish W, Miller W, Myers EW, Lipman DJ (1990) Basic local alignment search
539 tool Journal of molecular biology 215:403-410 doi:10.1016/s0022-2836(05)80360-2
540 Arif C et al. (2014) Assessing Symbiodinium diversity in scleractinian corals via next-
541 generation sequencing-based genotyping of the ITS2 rDNA region Mol Ecol 23:4418-
542 4433 doi:10.1111/mec.12869
543 Baird AH, Bhagooli R, Ralph PJ, Takahashi S (2009) Coral bleaching: the role of the host
544 Trends Ecol Evol 24:16-20 doi:10.1016/j.tree.2008.09.005
545 Baumgarten S et al. (2015) The genome of Aiptasia, a sea anemone model for coral
546 symbiosis Proc Natl Acad Sci U S A 112:11893-11898
547 doi:10.1073/pnas.1513318112
548 Belda-Baillie CA, Baillie BK, Maruyama T (2002) Specificity of a model cnidarian-
549 dinoflagellate symbiosis Biol Bull 202:74-85 doi:10.2307/1543224
550 Bellis ES, Denver DR (2017) Natural Variation in Responses to Acute Heat and Cold Stress
551 in a Sea Anemone Model System for Coral Bleaching Biol Bull 233:168-181
552 doi:10.1086/694890
553 Blanquet R, Lenhoff HM (1966) A disulfide-linked collagenous protein of nematocyst
554 capsules Science 154:152-153
555 Bolyen E et al. (2018) QIIME 2: Reproducible, interactive, scalable, and extensible
556 microbiome data science. PeerJ Preprints,
557 Bradford MM (1976) A rapid and sensitive method for the quantitation of microgram
558 quantities of protein utilizing the principle of protein-dye binding Analytical
559 biochemistry 72:248-254
560 Bucher M, Wolfowicz I, Voss PA, Hambleton EA, Guse A (2016) Development and
561 Symbiosis Establishment in the Cnidarian Endosymbiosis Model Aiptasia sp Sci Rep
562 6:19867 doi:10.1038/srep19867
563 Callahan BJ, McMurdie PJ, Rosen MJ, Han AW, Johnson AJA, Holmes SP (2016) DADA2:
564 high-resolution sample inference from Illumina amplicon data Nature methods 13:581
565 Carlisle JF, Murphy GK, Roark AM (2017) Body size and symbiotic status influence gonad
566 development in Aiptasia pallida anemones Symbiosis 71:121-127
567 doi:10.1007/s13199-016-0456-1
568 Chen C, Soong K, Chen CA (2008) The smallest oocytes among broadcast-spawning
569 actiniarians and a unique lunar reproductive cycle in a unisexual population of the
570 sea anemone, Aiptasia pulchella (Anthozoa : Actiniaria) Zool Stud 47:37-45
571 Cruz VM, Kilian A, Dierig DA (2013) Development of DArT marker platforms and genetic
572 diversity assessment of the U.S. collection of the new oilseed crop lesquerella and
573 related species PLoS One 8:e64062 doi:10.1371/journal.pone.0064062
574 Cunning R, Baker AC (2012) Excess algal symbionts increase the susceptibility of reef
575 corals to bleaching Nature Climate Change 3:259-262 doi:10.1038/nclimate1711
576 Cunning R, Baker AC (2014) Not just who, but how many: the importance of partner
577 abundance in reef coral symbioses Front Microbiol 5:400
578 doi:10.3389/fmicb.2014.00400
579 Cziesielski MJ, Liew YJ, Cui G, Schmidt-Roach S, Campana S, Marondedze C, Aranda M
580 (2018) Multi-omics analysis of thermal stress response in a zooxanthellate cnidarian
581 reveals the importance of associating with thermotolerant symbionts Proc Biol Sci
582 285 doi:10.1098/rspb.2017.2654
583 Damjanovic K, Blackall LL, Webster NS, van Oppen MJH (2017) The contribution of
584 microbial biotechnology to mitigating coral reef degradation Microbial biotechnology
585 10:1236-1243 doi:10.1111/1751-7915.12769
586 Davis RH (2004) The age of model organisms Nature Reviews Genetics 5:69
587 doi:10.1038/nrg1250
588 Davy SK, Allemand D, Weis VM (2012) Cell biology of cnidarian-dinoflagellate symbiosis
589 Microbiol Mol Biol Rev 76:229-261 doi:10.1128/MMBR.05014-11

De'ath G, Fabricius KE, Sweatman H, Puotinen M (2012) The 27-year decline of coral cover on the Great Barrier Reef and its causes Proc Natl Acad Sci U S A 109:17995-17999 doi:10.1073/pnas.1208909109

Duckworth CG, Picariello CR, Thomason RK, Patel KS, Bielmyer-Fraser GK (2017) Responses of the sea anemone, Exaiptasia pallida, to ocean acidification conditions and zinc or nickel exposure Aquat Toxicol 182:120-128 doi:10.1016/j.aquatox.2016.11.014

Eakin CM et al. (2016) Global Coral Bleaching 2014-2017 Status and an Appeal for Observations Reef Encounter 31:20-26

Fabricius K, De'ath G, McCook L, Turak E, Williams DM (2005) Changes in algal, coral and fish assemblages along water quality gradients on the inshore Great Barrier Reef Marine pollution bulletin 51:384-398

Fadlallah Y, Pearse J (1982) Sexual reproduction in solitary corals: overlapping oogenic and brooding cycles, and benthic planulas in Balanophyllia elegans Marine Biology 71:223-231

Falkowski PG, Dubinsky Z, Muscatine L, Mccloskey L (1993) Population-Control in Symbiotic Corals Bioscience 43:606-611 doi:Doi 10.2307/1312147

Franklin DJ, Hoegh-Guldberg O, Jones R, Berges JA (2004) Cell death and degeneration in the symbiotic dinoflagellates of the coral Stylophora pistillata during bleaching Marine Ecology Progress Series 272:117-130

Fransolet D, Roberty S, Plumier J-C (2014) Impairment of symbiont photosynthesis increases host cell proliferation in the epidermis of the sea anemone Aiptasia pallida Marine Biology 161:1735-1743 doi:10.1007/s00227-014-2455-1

Gates RD, Baghdasarian G, Muscatine L (1992) Temperature stress causes host cell detachment in symbiotic cnidarians: implications for coral bleaching The Biological Bulletin 182:324-332

Goffredo S et al. (2012) Unusual pattern of embryogenesis of Caryophyllia inornata (scleractinia, caryophylliidae) in the mediterranean sea: Maybe agamic reproduction? Journal of morphology 273:943-956

Goyen S, Pernice M, Szabó M, Warner ME, Ralph PJ, Suggett DJ (2017) A molecular physiology basis for functional diversity of hydrogen peroxide production amongst Symbiodinium spp.(Dinophyceae) Marine biology 164:46

Grajales A, Rodriguez E (2014) Morphological revision of the genus Aiptasia and the family Aiptasiidae (Cnidaria, Actiniaria, Metridioidea) Zootaxa 3826:55-100 doi:10.11646/zootaxa.3826.1.2

Grajales A, Rodriguez E (2016) Elucidating the evolutionary relationships of the Aiptasiidae, a widespread cnidarian-dinoflagellate model system (Cnidaria: Anthozoa: Actiniaria: Metridioidea) Mol Phylogenet Evol 94:252-263 doi:10.1016/j.ympev.2015.09.004

Grawunder D, Hambleton EA, Bucher M, Wolfowicz I, Bechtoldt N, Guse A (2015) Induction of Gametogenesis in the Cnidarian Endosymbiosis Model Aiptasia sp Sci Rep 5:15677 doi:10.1038/srep15677

Gruber B, Georges A, Berry O, Unmack P (2017) dartR: Importing and Analysing Snp and Silicodart Data Generated by Genome-Wide Restriction Fragment Analysis. CRAN,

Hawkins TD, Hagemeyer JC, Warner ME (2016a) Temperature moderates the infectiousness of two conspecific Symbiodinium strains isolated from the same host population Environmental microbiology 18:5204-5217

Hawkins TD, Hagemeyer JCG, Hoadley KD, Marsh AG, Warner ME (2016b) Partitioning of Respiration in an Animal-Algal Symbiosis: Implications for Different Aerobic Capacity between Symbiodinium spp Frontiers in Physiology 7:128 doi:10.3389/fphys.2016.00128

Hillyer KE, Dias DA, Lutz A, Roessner U, Davy SK (2017) Mapping carbon fate during bleaching in a model cnidarian symbiosis: the application of 13 C metabolomics New Phytol 214:1551-1562 doi:10.1111/nph.14515

Hoadley KD, Rollison D, Pettay DT, Warner ME (2015) Differential carbon utilization and asexual reproduction under elevatedpCO2conditions in the model

anemone,Exaiptasia pallida, hosting different symbionts Limnology and Oceanography 60:2108-2120 doi:10.1002/lno.10160

Hoadley KD, Warner ME (2017) Use of Open Source Hardware and Software Platforms to Quantify Spectrally Dependent Differences in Photochemical Efficiency and Functional Absorption Cross Section within the Dinoflagellate Symbiodinium spp Frontiers in Marine Science 4 doi:10.3389/fmars.2017.00365

Hothorn T, Bretz F, Westfall P, Heiberger RM, Schuetzenmeister A, Scheibe S, Hothorn MT (2016) Package 'multcomp' Simultaneous inference in general parametric models Project for Statistical Computing, Vienna, Austria

Howe PL, Reichelt-Brushett AJ, Clark MW, Seery CR (2017) Toxicity estimates for diuron and atrazine for the tropical marine cnidarian Exaiptasia pallida and in-hospite Symbiodinium spp. using PAM chlorophyll-a fluorometry J Photochem Photobiol B 171:125-132 doi:10.1016/j.jphotobiol.2017.05.006

Howells E, Beltran V, Larsen N, Bay L, Willis B, Van Oppen M (2012) Coral thermal tolerance shaped by local adaptation of photosymbionts Nature Climate Change 2:116

Hughes TP et al. (2017) Global warming and recurrent mass bleaching of corals Nature 543:373-377 doi:10.1038/nature21707

Hughes TP et al. (2018) Global warming transforms coral reef assemblages Nature 556:492-496 doi:10.1038/s41586-018-0041-2

ICZN (2017) Opinion 2404 (Case 3633) —Dysactis pallida Agassiz in Verrill, 1864 (currently Aiptasia pallida; Cnidaria, Anthozoa, Hexacorallia, Actiniaria): precedence over Aiptasia diaphana (Rapp, 1829), Aiptasia tagetes (Duchassaing de Fombressin & Michelotti, 1864), Aiptasia mimosa (Duchassaing de Fombressin & Michelotti, 1864) and Aiptasia inula (Duchassaing de Fombressin & Michelotti, 1864) not approved The Bulletin of Zoological Nomenclature 74:130-132, 133

Kearse M et al. (2012) Geneious Basic: an integrated and extendable desktop software platform for the organization and analysis of sequence data Bioinformatics (Oxford, England) 28:1647-1649 doi:10.1093/bioinformatics/bts199

Kenkel CD, Bay LK (2018) Exploring mechanisms that affect coral cooperation: symbiont transmission mode, cell density and community composition bioRxiv:067322 doi:10.1101/067322

Kumar S, Stecher G, Li M, Knyaz C, Tamura K (2018) MEGA X: molecular evolutionary genetics analysis across computing platforms Molecular biology and evolution 35:1547-1549

LaJeunesse TC, Parkinson JE, Gabrielson PW, Jeong HJ, Reimer JD, Voolstra CR, Santos SR (2018) Systematic Revision of Symbiodiniaceae Highlights the Antiquity and Diversity of Coral Endosymbionts Curr Biol 28:2570-2580 e2576 doi:10.1016/j.cub.2018.07.008

Lehnert EM, Burriesci MS, Pringle JR (2012) Developing the anemone Aiptasia as a tractable model for cnidarian-dinoflagellate symbiosis: the transcriptome of aposymbiotic A. pallida BMC Genomics 13:271 doi:10.1186/1471-2164-13-271

Lehnert EM, Mouchka ME, Burriesci MS, Gallo ND, Schwarz JA, Pringle JR (2014) Extensive differences in gene expression between symbiotic and aposymbiotic cnidarians G3 (Bethesda) 4:277-295 doi:10.1534/g3.113.009084

Melville J et al. (2017) Identifying hybridization and admixture using SNPs: application of the DArTseq platform in phylogeographic research on vertebrates Royal Society open science 4:161061

Muller-Parker G, Cook CB, D'Elia CF (1990) Feeding affects phosphate fluxes in the symbiotic sea anemone Aiptasia pallida Marine Ecology Progress Series 60:283-290

Muscatine L, Porter JW (1977) Reef corals: mutualistic symbioses adapted to nutrient-poor environments Bioscience 27:454-460

Nei M, Kumar S (2000) Molecular evolution and phylogenetics. Oxford university press,

O'Mahony J, Simes R, Redhill D, Heaton K, Atkinson C, Hayward E, Nguyen M (2017) At what price? The economic, social and icon value of the Great Barrier Reef. Deloitte Access Economics, Brisbane, QLD, Australia

Perez SF, Cook CB, Brooks WR (2001) The role of symbiotic dinoflagellates in the temperature-induced bleaching response of the subtropical sea anemone Aiptasia pallida Journal of Experimental Marine Biology and Ecology 256:1-14

Pinheiro J, Bates D, DebRoy S, Sarkar D, Heisterkamp S, Van Willigen B, Maintainer R (2017) Package 'nlme' Linear and Nonlinear Mixed Effects Models, version:3-1

Pochon X, Pawlowski J, Zaninetti L, Rowan R (2001) High genetic diversity and relative specificity among Symbiodinium-like endosymbiotic dinoflagellates in soritid foraminiferans Marine Biology 139:1069-1078 doi:10.1007/s002270100674

Rädecker N et al. (2018) Using Aiptasia as a Model to Study Metabolic Interactions in Cnidarian-Symbiodinium Symbioses Frontiers in physiology 9:214-214 doi:10.3389/fphys.2018.00214

Ragni M, Airs RL, Hennige SJ, Suggett DJ, Warner ME, Geider RJ (2010) PSII photoinhibition and photorepair in Symbiodinium (Pyrrhophyta) differs between thermally tolerant and sensitive phylotypes Marine Ecology Progress Series 406:57-70

Rapp W (1829) Über die Polypen im Allgemeinen und die Actinien Verlag des Großherzoglich Sächsischen privileg Landes-Industrie-Comptoirs, Weimar

Rognes T, Flouri T, Nichols B, Quince C, Mahé F (2016) VSEARCH: a versatile open source tool for metagenomics PeerJ 4:e2584

Rohwer F, Seguritan V, Azam F, Knowlton N (2002) Diversity and distribution of coral-associated bacteria Mar Ecol Prog Ser 243:10

Rosado PM et al. (2018) Marine probiotics: increasing coral resistance to bleaching through microbiome manipulation The ISME Journal doi:10.1038/s41396-018-0323-6

Schlesinger A, Kramarsky-Winter E, Rosenfeld H, Armoza-Zvoloni R, Loya Y (2010) Sexual plasticity and self-fertilization in the sea anemone Aiptasia diaphana PLoS One 5:e11874 doi:10.1371/journal.pone.0011874

Stat M, Pochon X, Cowie RO, Gates RD (2009) Specificity in communities of Symbiodinium in corals from Johnston Atoll Marine Ecology Progress Series 386:83-96

Steele RD (1976) Light intensity as a factor in the regulation of the density of symbiotic zooxanthellae in Aiptasia tagetes (Coelenterata, Anthozoa) Journal of Zoology 179:387-405 doi:doi:10.1111/j.1469-7998.1976.tb02302.x

Suggett DJ, Warner ME, Smith DJ, Davey P, Hennige S, Baker NR (2008) Photosynthesis and production of hydrogen peroxide by Symbiodinium (pyrrhophyta) phylotypes with different thermal tolerances 1 Journal of Phycology 44:948-956

Sunagawa S et al. (2009) Generation and analysis of transcriptomic resources for a model system on the rise: the sea anemone Aiptasia pallida and its dinoflagellate endosymbiont BMC Genomics 10:258 doi:10.1186/1471-2164-10-258

Team RC (2013) R: A language and environment for statistical computing

Thornhill DJ, Xiang Y, Pettay DT, Zhong M, Santos SR (2013) Population genetic data of a model symbiotic cnidarian system reveal remarkable symbiotic specificity and vectored introductions across ocean basins Mol Ecol 22:4499-4515 doi:10.1111/mec.12416

Verrill AE Revision of the polypi of the eastern coast of the United States. In, 1864. Boston Society of Natural History,

Wangpraseurt D, Larkum AW, Franklin J, Szabo M, Ralph PJ, Kuhl M (2014) Lateral light transfer ensures efficient resource distribution in symbiont-bearing corals J Exp Biol 217:489-498 doi:10.1242/jeb.091116

Weis VM, Davy SK, Hoegh-Guldberg O, Rodriguez-Lanetty M, Pringle JR (2008) Cell biology in model systems as the key to understanding corals Trends Ecol Evol 23:369-376 doi:10.1016/j.tree.2008.03.004

751 Wilson K et al. (2002) Genetic mapping of the black tiger shrimp Penaeus monodon with
752 amplified fragment length polymorphism Aquaculture 204:297-309
753 doi:https://doi.org/10.1016/S0044-8486(01)00842-0
754 Xiang T, Hambleton EA, DeNofrio JC, Pringle JR, Grossman AR (2013) Isolation of clonal
755 axenic strains of the symbiotic dinoflagellate Symbiodinium and their growth and host
756 specificity(1) J Phycol 49:447-458 doi:10.1111/jpy.12055
757 Ziegler M, Roder CM, Büchel C, Voolstra CR (2015) Mesophotic coral depth acclimatization
758 is a function of host-specific symbiont physiology Frontiers in Marine Science 2:4
759